—Original Article—

In Vivo Measurements of Flexor Tendon and Suspensory Ligament Forces During Trotting Using the Thoroughbred Forelimb Model

Toshiyuki TAKAHASHI*, Kazutaka MUKAI, Hajime OHMURA, Hiroko AIDA and Atsushi HIRAGA

Sport Science Division, Equine Research Institute, Japan Racing Association, Tochigi 320-0856, Japan

The purpose of this study was to create a lower forelimb model of the Thoroughbred horse for measuring the force in the superficial and deep digital flexor tendons (SDFT and DDFT), and the suspensory ligament (SL) during a trot. The mass, centers of gravity, and inertial moments in the metacarpus, pastern, and hoof segments were measured in 4 Thoroughbred horses. The moment arms of the SDFT, DDFT, and SL in the metacarpophalangeal (fetlock) and distal interphalangeal (coffin) joints were measured in 7 Thoroughbred horses. The relationship between the fetlock joint angle and the force in the SL was assessed in 3 limbs of 2 Thoroughbred horses. The forces in the SDFT, DDFT, and SL during a trot were also measured in 7 Thoroughbred horses. The mass of the 3 segments, and the moment arms of the SDFT and DDFT in the fetlock joint of the Thoroughbred horses were smaller than those the Warmblood horses, whereas the other values were almost the same in the 2 types. The calculated force in the SDFT with this Thoroughbred model reached a peak (4,615 N) at 39.3% of the stance phase, whereas that in the DDFT reached a peak (5,076 N) at 51.2% of the stance phase. The force in the SL reached a peak (11,957 N) at 49.4% of the stance phase. This lower forelimb model of the Thoroughbred can be applied to studying the effects of different shoe types and change of hoof angle for the flexor tendon and SL forces.
Key words: *segment center of gravity, inertial moment, Thoroughbred, inverse dynamics, tendon*

Injuries of the forelimb flexor tendons and ligaments, especially those of the superficial digital flexor tendon (SDFT), deep digital flexor tendon (DDFT), and the suspensory ligament (SL), are a common occurrence in athletic horses [9, 13, 14, 32]. Although the causes of these injuries have not been clearly specified, the overload or repeated loading of the tendons and the ligaments is assumed to be one of them [7, 8, 31]. Therefore, measuring the load in the tendons and the ligaments is useful for the prevention and treatment of these injuries. The forces in the tendons and ligaments have been previously measured by invasive methods such as inserting a strain or force sensor into each tendon or ligament [3, 12, 17, 23, 26–30]. However, the problems with this method were low durability of the sensors and a low success rate. Moreover, because the sensors are inserted into the tendon or ligament, the insertion sites are easily damaged and can be used only once, making multiple repetitions of the experiment difficult. Although a new noninvasive method using ultrasonic transfer speed has been developed recently for measuring these forces [5, 6, 24], it can be used only for the SDFT and not for the DDFT or SL.

In humans, the tendon and ligament forces are measured by using noninvasive inverse dynamics [10], and this is also used in horses during walking, trotting, and jumping [12, 18–20]. It requires the development of a model from the anatomical data obtained from other horses, the data from a motion analysis system, and the ground reaction force

(GRF). However, the models reported until now have been those of a large horse like a Warmblood or a small pony [2, 21], both of which are different from the Thoroughbred racehorses in body weight (*M*) and configuration.

The purpose of this study was to create the lower fore-limb model of a Thoroughbred and measure the forces in the SDFT, DDFT, and SL during a trot using this model.

Materials and Methods

Model formulation in the lower forelimb

1. The measurement of the moment arms

The left forelimbs of 7 Thoroughbred horses (5 males, 2 females; mean ± SD: *M*, 460 ± 22 kg; age, 6.6 ± 2.1 years) were obtained from necropsy specimens dissected for reasons other than this experiment. The forelimbs were cut at the middle of the radius and frozen at –20°C until the measurements were performed.

The frozen limbs were sectioned in the median plane. The photograhps of the metacarpophalangeal (fetlock joint) and the distal interphalangeal joints (coffin joint) were taken with the reference length and the positions of the center of rotation and the moment arms were measured from photographs using software (ImageJ 1.43u) [1]. The positions of the center of rotation at the fetlock joint and the coffin joint were determined by fitting the circle to the arc of each joint. The moment arm was determined to be the minimum length from the center of the joint to the SDFT, DDFT, or SL. The resolution was about 130 pixels/cm.

The statistical significance of the regression models between the moment arm and *M* was set as P<0.05 using the Pearson's correlation coefficient (JMP 9.0.3, SAS Institute, Cary, North Carolina, USA) .

2. The relationship between the fetlock joint angle and the force in the suspensory ligament

Three forelimbs from 2 male Thoroughbred horses (*M*, 445 and 515 kg; age, 6 and 8 years) were obtained from necropsy specimens dissected for reasons other than this experiment. The forelimbs were cut at the distal part of radius and stored frozen at –20°C until the measurements were performed; they were thawed overnight. During the experiments, the SL was maintained in a wet state with saline solution.

The relationship between the fetlock joint angle and SL strain, and the relationship between the SL strain and force were determined with the modified method in a previously conducted study [22]. The skin over the metacarpal area, the SDFT, and DDFT were removed. Two markers for the video extensometer were glued on the palmar surface of the SL at a mutual distance of approximately 3 cm. Three markers (1 cm in diameter) were glued on the lateral side of the

specimen at the center of the fetlock and coffin joints, and at the middle between the center of the carpus and fetlock joint, to measure the fetlock joint angle. The hoof was fixed to the horizontal plate connected to the universal testing machine (AG-IS 100kN, SHIMADZU CORPORATION, Kyoto, Japan). The limb was loaded on the radius to 2.0 kN and unloaded to 0.2 kN. The vertical GRF (VGRF) at trot was reported about 5.0 to 6.0 kN in 400 to 500 kg body weight horses [4,19]. Because SDFT and DDFT that supported the moment of the fetlock joint with SL were removed specimen, the maximum vertical load was reduced to 2.0 kN. This was repeated 10 times at a head speed of 35 or 70 mm/min. The SL strain was measured by the video extensometer (DVE-201, SHIMADZU CORPORATION) at a sample frequency of 100 Hz. The fetlock joint angle was measured by the 1-camera high-speed video system (HSV-500C3. nac Image Technology Inc., Tokyo, Japan) at a sample frequency of 250 Hz. The start time of these systems was synchronized by an electronic flash of LED. The motion data were resampled at a frequency of 6.25 Hz, because data at one cycle were too many and enough data points were taken at a low sampling rate (about 180 points at one cycle). The fetlock joint angle was determined by the motion analysis system (Movias, nac Image Technology Inc., Tokyo, Japan). The data of SL strain that were at the closest time points to those of the fetlock joint angle data were used for analysis. The tenth uploading data were used to determine the angle–SL strain relationship by fitting linear regression equations. The slopes in these equations were averaged to obtain the mean value.

After measuring the relationship between the fetlock joint angle and SL strain, the SL, including the sesamoid bone and the distal sesamoidean ligament, was removed from the bone without removing the glued markers. SL was clamped in the cryo-jaws [25] for the ligament-loading experiments to determine the strain-force relationship of SL. The SL was loaded to 4.0 kN and unloaded to 0.3 kN. This cycle was repeated 10 times at a head speed of 100 or 200 mm/min (AG-IS 100kN, SHIMADZU CORPORATION). The maximum SL force at trot was reported about 12.0 kN in about 500 kg body weight horses [4, 19]. However, maximum load was set at 4.0 kN, because our cryo-jaws could not hold the SL over 4.0 kN without fault. The SL strain and force were measured by the video extensometer (DVE-201, SHIMADZU CORPORATION) and the load cell (AG-IS 100kN, SHIMADZU CORPORATION) at a sample frequency of 100 Hz. The tenth uploading data were used to determine the SL strain–SL force relationship by fitting linear regression equations. The slopes of linear regression equations were averaged to obtain the mean value. The slope of the fetlock joint angle–SL strain and the SL strain–SL force relationship were used to calculate

the slope of the fetlock joint angle–force relationship.

3. The measurement of the center of gravity and the inertial moment in the metacarpus, pastern, and hoof segments

The left forelimbs of 4 Thoroughbred horses (3 males, 1 female; mean ± SD: M, 447 ± 82 kg; age, 5.3 ± 1.3 years) were obtained from necropsy specimens dissected for reasons other than this experiment. The forelimbs were cut at the distal part of the radius and stored frozen at –20°C until the experiments.

The definition of the lower limb segment was similar to that described by Buchner *et al.* [2] (Fig. 1). The limb was cut in the middle of the proximal carpal bones, the center of the fetlock and coffin joints. In this model, the proximal interphalangeal joint was assumed to be fixed.

The centers of gravity and the inertial moments in the metacarpus, pastern, and hoof segments were measured by the method described in a previous report [2, 16]. The center of gravity and inertial moment were expressed relative to a segment-based coordinate system (Fig. 1). The origin of this coordinate system was the lateral projection of the center of the proximal joint. In the metacarpus and the pastern segments, the x-axis ran through the lateral projection of the center of the distal joint. In the hoof segment, the definition of the x-axis was modified. The x-axis was perpendicular to the sole of the hoof. In all segments, the z-axis was perpendicular to the x-axis and pointed medially. The XZ plane contained the medial projection of the center of the proximal joint. The y-axis was perpendicular to the XZ plane and pointed cranially. The x-axis was defined as a reference line. The reference length L was the distance between the lateral projection of the center of the proximal and distal joints in the metacarpus and the pastern segments. In the hoof segment, it was the height of the projection at the center of the coffin joint from the hoof sole.

An aluminum fixation (weight, 2.634 kg) was built, and the center of mass and the inertial tensor of the segments were determined according to the method described by Lephart [16]. Oscillation times of box-segment units were measured around 6 axes. The time for 20 complete oscillations was determined using a laser displacement meter (LB-01 + LB-60 and KZ-U3, response speed 0.7 ms, KEYENCE CORPORATION, Osaka, Japan) and recording software (DI-720 and WinDaq/Pro+, DATAQ, Akron, Ohio, USA) at a sampling frequency of 1,000 Hz to calculate the time for one oscillation. The complete inertial tensor with respect to the segment's center of gravity was calculated.

Regression models were used to test the relationships among M, segment mass (m), moment of inertia, and L. Two different models for m and moments of inertia around the 3 principal segment axes (I_{xx}, I_{yy}, I_{zz}) were tested as described in a previously published report [2]. For estimation of m, the M or the L was used. For estimation of the moment of
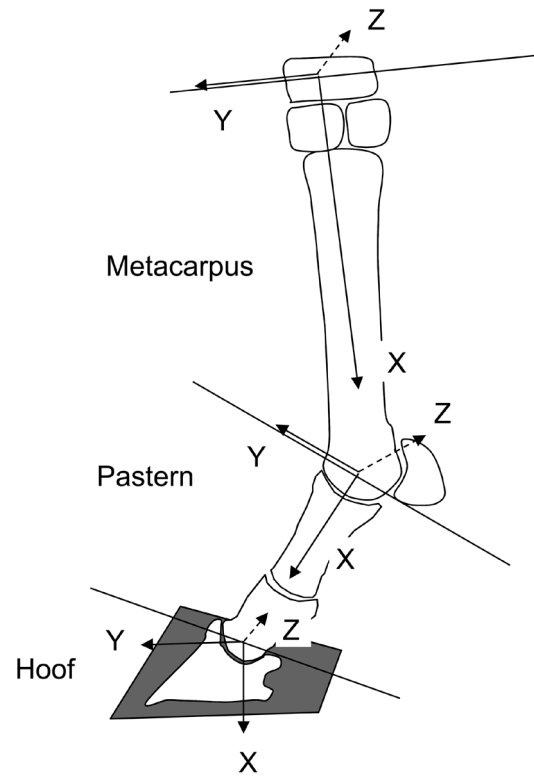

Fig. 1. Local reference frame in lower forelimb.

inertia, the product of m and squared L (mL^2) or L were used. Significance level was set at P<0.05. When both models were significant, the model in which the correlation coefficient was higher was selected (JMP 9.0.3).

The measurement of force in the superficial and deep digital flexor tendons, and the suspensory ligament during a trot

These measurements were conducted as part of another experiment [30]. Seven Thoroughbred horses (3 males, 2 females, and 2 geldings; mean ± SD: M, 520 ± 24 kg; age, 3–7 years) were used. All horses were confirmed as not being lame and did not wear shoes for the experiments. One horse participated in 2 experiments using either the left or the right limb each time. The experiments for the 2 sides were conducted at different times. In the other 6 horses, the data of 1 experiment with the left or right limb were used to calculate the force in the tendons and the SL. Data were obtained on a total of 8 limbs.

Four markers (1 cm in diameter) were attached to the hoof (lateral at widest hoof width) and the centers of rotation of each joint. The positions of the distal interphalangeal (coffin), metacarpophalangeal (fetlock), and carpal joints relative to the markers were confirmed by radiographs. Kinematic measurements were performed with the use of the

Table 1. Characteristics and length of moment arms at the fetlock and coffin joints in the 7 Thoroughbred horses

| Horse | Sex | M (kg) | Age (years) | The moment arms (mm) | | | |
| | | | | Fetlock joint | | | Coffin joint |
				SL	DDFT	SDFT	DDFT
A	Female	451	6	28.2	39.4	47.8	28.4
B	Male	475	4	31.7	42.8	50.2	29.5
C	Male	488	4	28.4	39.4	46.5	29.5
D	Male	451	7	33.4	44.4	51.4	31.7
E	Female	444	9	30.0	40.1	47.5	30.8
F	Male	482	9	29.4	40.7	49.0	30.9
G	Male	429	7	29.2	38.7	46.4	29.6
Mean		460	6.6	30.0	40.8	48.4	30.1
Standard deviation		22	2.1	1.9	2.1	1.9	1.1

Mean moment arms are cited from a previous report [30]. M=body weight; SL=suspensory ligament; DDFT=deep digital flexor tendon; SDFT=superficial digital flexor tendon.

2D motion analysis system with one camera (HSV-500C3, nac Image Technology Inc.), and the GRF was measured by the force plate (DPM-612B and EFP-396ASA21, Kyowa Electronic Instruments, Tokyo, Japan). The skin movement artifact was not corrected because the skin displacement in the distal parts of the limb is small. The horses trotted at a comfortable speed (approximately 3 m/s) during the kinematic and GRF measurements. All signals and kinematic data were synchronized and recorded at 250 Hz on a data recording system (ADM-686z PCI and LaBDAQ PRO, MICRO SCIENCE, Chiba, Japan).

Tendon and ligament forces were calculated using the method reported previously [18, 22]. However, the mean values of m and the moment of inertia measured in this study for the Thoroughbred were used for the *in vitro* model of the forelimb (Tables 1 and 2). The L in each segment was calculated from the results of the 2D motion analysis, and the center of mass was calculated from the percentage of L (Table 2). The time when GRF reached 200 N was defined as ground contact, and the force in the SL was assumed to be 0 at that time. Kinematics was analyzed by software (MOVIAS, resolution was about 5 pixels/cm, nac Image Technology Inc.) and data were filtered using a low-pass filter (second order, 15 Hz recursive Butterworth filter). The positions and accelerations of the segments' center of gravity were calculated from the filtered data and the model developed in this study.

With the help of software (BIMUTUS, KISSEI COMTEC CO., LTD., Nagano, Japan), the peak values and times of the VGRF, SDFT, DDFT, and SL were determined. These data were also normalized to 100% stance phase duration and the mean values and standard errors were calculated using the same software (BIMUTUS).

All procedures were approved by the Equine Research Institute's Animal Care and Use Committee.

Results

Forelimb model

The M and moment arms are represented in Table 1. There was no correlation between M and the moment arms. The mean of the slope of the fetlock joint angle-SL strain, the SL strain-SL force, and the fetlock joint angle-SL force relationships were 0.202%/degree, 1568.4 N/%, and 311.5 N/degree, respectively [30]. The m, segment length, and the position of the segment's center of mass along the 3 segmental axes are represented in Table 2. M and m were correlated in all segments. The mL^2 and the moment of inertia around the y- and z-axes were also correlated in the metacarpus segment (Table 3).

Calculated flexor tendon and suspensory ligament forces

The peak values and times for each force are represented in Table 4. VGRF reached a peak at early middle of the stance phase. The force in the SDFT was approximately 0 during the initial 5% of the stance phase, and then increased to reach a peak earlier than VGRF (Table 4 and Fig. 2). In the final 30% of the stance phase, it assumed a negative value (Fig. 2). The force in the DDFT reached a peak at the middle of the stance phase, then decreased and increased slowly to reach a second peak at approximately 85% of the stance phase (Table 4 and Fig. 2). The force in the SL reached a peak at the middle of the stance phase (Table 4 and Fig. 2).

Table 2. Mass (*m*), reference length (*L*), center of mass (CoM), moment of inertia (*I*), and product of inertia (*P*) for the segments of the Thoroughbred model

Segment	m (kg)	L (m)	CoM_x (%)	CoM_y (%)	CoM_z (%)	I_{xx} (kg m^2)	I_{yy} (kg m^2)	I_{zz} (kg m^2)	P_{xy} (kg m^2)	P_{yz} (kg m^2)	P_{xz} (kg m^2)
Metacarpus	1.435	0.299	44.2	–2.7	15.3	0.00125	0.01448	0.01479	–0.00050	0.00028	–0.00027
	(0.300)	(0.019)	(1.2)	(0.9)	(0.5)	(0.0004)	(0.00388)	(0.00414)	(0.00040)	(0.00035)	(0.00026)
Pastern	0.605	0.131	47.5	–6.6	26.8	0.00043	0.00204	0.00201	0.00044	–0.00014	0.00022
	(0.137)	(0.009)	(2.1)	(7.1)	(2.7)	(0.00020)	(0.00073)	(0.00076)	(0.00018)	(0.00072)	(0.00010)
Hoof	0.704	0.066	53.9	8.1	68.5	0.00174	0.00113	0.00091	0.00038	0.00011	0.00033
	(0.117)	(0.007)	(2.3)	(10.7)	(14.5)	(0.00057)	(0.00045)	(0.00029)	(0.00043)	(0.00023)	(0.00012)

CoM_x, CoM_y and CoM_z are the x, y, and z locations of the percentage of segment length of the center of mass in the local reference frame. I_{xx}, I_{yy}, and I_{zz} is the segment moment of inertia, and P_{xx}, P_{yy}, and P_{zz} is the segment product of inertia about the x-, y-, and z-axes at the segment's CoM. Data are expressed as mean (standard deviation). m and I_{zz} in 3 segments, and CoM_x and CoM_y in the metacarpus and pustern segment are cited from a previous report [30].

Table 3. Significant regression models, correlation coefficient (r), and coefficient of determination (R^2)

Segment	Regression equation	r	R^2
	$m = 0.003552M - 0.1530$	0.969	0.938
Metacarpus	$I_{yy} = 0.08549mL^2 + 0.003271$	0.995	0.989
	$I_{zz} = 0.09145mL^2 + 0.002807$	0.996	0.991
Pastern	$m = 0.001635M - 0.1263$	0.978	0.956
Hoof	$m = 0.001411M + 0.0737$	0.988	0.976

Table 4. Maximum force and peak time in the vertical ground reaction force (VGRF), suspensory ligament (SL), superficial digital flexor tendon (SDFT), and deep digital flexor tendon (DDFT) during a trot

	VGRF	SL	SDFT	DDFT
Maximum force (N)	5,528	11,957	4,615	5,076
	(395)	(1,608)	(1,359)	(1,823)
Peak time (%stance)	44.7	49.4	39.3	51.2
	(3.7)	(3.4)	(4.0)	(5.1)

Data (N=8) are expressed as mean (standard deviation).

Fig. 2. Calculated mean force of superficial digital flexor tendon (SDFT), deep digital flexor tendon (DDFT), and suspensory ligament (SL) during a trot. The thin lines represent values of ± 1 standard error of the mean value.

Discussion

In this study, forces were calculated by applying an *in vitro* model of the distal portion of the forelimb to inverse dynamic data. These forces are influenced by several sources of errors such as measurement errors in the force plate and motion analysis system, the inaccuracy in the joint center positions, the interindividual difference of inertial properties, moment arms, and the relationship between force in the SL and the fetlock joint angle. The influence of these error sources has been discussed in detail elsewhere [18]. Briefly, a major source of errors is the distance between the application point of GRF and the center of the coffin joint. However, in this study, it was confirmed that the error of the application point of GRF w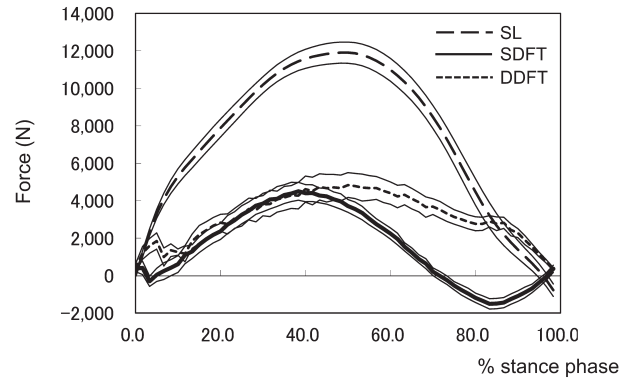as less than 1 cm, and the marker position of the coffin joint was on the center of rotation by radiography. In previous reports on calculation of the forces in these tendons and the SL, the data used were that of a large horse like the Warmblood [22] or a small pony [11]. Because a Thoroughbred is different from a Warmblood or a pony in *M* and configuration, the force in the SL-angle of the fetlock joint relationship, inertial properties, and the moment arms might differ. Therefore, a lower limb model of the Thoroughbred was developed in this study.

The definition of the lower limb segment was similar to that described by Buchner *et al.* [2] (Fig. 1) to compare the results between Warmblood and Thoroughbred. The proximal interphalangeal joint was also assumed to be fixed. It was reported that the fixation of the proximal interphalangeal joint in the model affected the strains in SDFT, DDFT and SL at a trot [15]. However, the fixation of this joint seemed to have small effects.

Although the Thoroughbred horses used in this study had lesser *M* than the Warmblood horses, on whom previous

reports have been based, the *L* and the position of the segment's center of mass along the 3 segmental axes in the metacarpus and pastern segments were of almost the same value [2]. However, the *m* of the metacarpus, pastern, and hoof segments was smaller than that in the Warmblood [2]. Furthermore, because the definitions of the 3 axes and the *L* of the hoof segment in this study were different from those of previous reports [18], the position of the segment's center of the mass and inertial properties were different [2]. The moment arms of the SDFT and DDFT in the fetlock joint were smaller than those in a previous report on larger horses weighing >500 kg [22], whereas the moment arm of the SL in the fetlock joint did not differ. The moment arm of the DDFT in the coffin joint was different because of the difference in the definition of the center of rotation [22].

The regression analysis revealed significant relationships between the inertial moment in the metacarpus segment and *m* in all segments. These results were similar to those of a previous report [2]. However, these relationships should be used with appropriate caution because these data were calculated from the data of only 4 horses. In substitution for the values calculated from the regression formula, the mean values of *m* and the moment inertia were used to calculate the forces in the tendons and the SL during the stance phase in this study. However, the influence of the errors in *m* and the inertial properties might not be large because the motion in these segments during the stance phase was not too fast. Furthermore, the moment arm of the tendons and the SL had no correlation with *M*. Therefore, the mean values of these parameters were used in this study to calculate the forces in the tendons and SL during the stance phase.

It was reported that the large inaccuracies are caused by errors in the SL model [18]. The fetlock joint angle–SL force relationship and the definition of zero-angle of the fetlock joint have a large influence on accuracy in this model. It is difficult to correct the angle–force relationship because this error originates from the interindividual variation in the SL property. However, the variation of the SL force at impact could be reduced by defining the angle of the fetlock joint at impact as zero. Variation can also be reduced by using the difference of fetlock joint angle at impact to calculate the SL force.

The angle of the fetlock joint-SL strain, SL strain-SL force, and the angle of the fetlock joint–SL force relationships were determined at a slow speed rather than at normal speed during a trot. Although the force or strain at failure changes depending on the strain rate, the modulus of the tendon and SL is not significantly affected [33, 34]. The strain rate has a small effect on the calculated force in the flexor tendons and SL.

As reported in a previous study [18, 19], the force in the SDFT and SL peaked around the midstance phase. However, the peak values of the force in the SDFT and SL were lower than those in the previous reports [18, 19]. The force in the DDFT peaked later, and the peak value was higher than that in the SDFT. These results were different from those of previous reports [18, 19], whereas the peak value was not different. The mean *M* of the horses used in this experiment was similar to that of the horses used in previous studies, whereas the VGRF in this study (10.6 N/kg) was lower than that in the previous study (12.3 N/kg) [4, 19]. This difference may be related to the lower peak values of the force in the SL and SDFT in this study. However, the difference in the breeds (conformation and kinematics) used in this study and the previous study is assumed to have affected the calculated force in the tendons and SL because the peak time and value of the force in the DDFT were also different in this study.

The force in the SDFT in the final 30% assumed a negative value in this study, whereas it was 0 in the final 20% in the previous report [5, 15, 18]. During this time, the coffin joint is hyperextended, and the navicular ligaments are strained and generate part of the net coffin joint moment. The force in the DDFT is therefore overestimated and the force in the SDFT is underestimated [20]. These errors might have an effect on the calculated force in the SDFT. On the other hand, the early disappearance of the SDFT force was in agreement with a previous report, in which the SDFT force was measured by an implanted probe in Thoroughbred horses [30]. This discrepancy may be attributed to the differences in conformation, running form, or the *in vitro* distal forelimb model used.

It was possible to calculate the forces in the SDFT, DDFT, and SL noninvasively during a trot with inverse dynamics and the Thoroughbred lower forelimb model reported in this study. It was not possible to evaluate the force in the flexor tendon and suspensory ligament between individual horses because this forelimb model of the Thoroughbred includes the error from interindividual variation. However, it can be used for studying the effects of different shoe types and change of hoof angle and equipment on the joint moments by comparing the forces in the flexor tendons and SL in the same horse.

References

1. Abramoff, M.D., Magelhaes, P.J., and Ram, S.J. 2004. Image processing with ImageJ. *Biophotonics Int.* **11**: 36–42.
2. Buchner, H.H., Savelberg, H.H., Schamhardt, H.C., and Barneveld, A. 1997. Inertial properties of Dutch Warmblood horses. *J. Biomech.* **30**: 653–658. [Medline] [CrossRef]
3. Butcher, M.T., Hermanson, J.W., Ducharme, N.G., Mitchell, L.M., Soderholm, L.V., and Bertram, J.E. 2007. Superficial digital flexor tendon lesions in racehorses as a

sequela to muscle fatigue: a preliminary study. *Equine Vet. J.* **39**: 540–545. [Medline] [CrossRef]

4. Clayton, H.M., Schamhardt, H.C., Willemen, M.A., Lanovaz, J.L., and Colborne, G.R. 2000. Kinematics and ground reaction forces in horses with superficial digital flexor tendinitis. *Am. J. Vet. Res.* **61**: 191–196. [Medline] [CrossRef]

5. Crevier-Denoix, N., Pourcelot, P., Ravary, B., Robin, D., Falala, S., Uzel, S., Grison, A.C., Valette, J.P., Denoix, J.M., and Chateau, H. 2009. Influence of track surface on the equine superficial digital flexor tendon loading in two horses at high speed trot. *Equine Vet. J.* **41**: 257–261. [Medline] [CrossRef]

6. Crevier-Denoix, N., Ravary-Plumioën, B., Evrard, D., and Pourcelot, P. 2009. Reproducibility of a non-invasive ultrasonic technique of tendon force measurement, determined in vitro in equine superficial digital flexor tendons. *J. Biomech.* **42**: 2210–2213. [Medline] [CrossRef]

7. Dowling, B.A., and Dart, A.J. 2005. Mechanical and functional properties of the equine superficial digital flexor tendon. *Vet. J.* **170**: 184–192. [Medline] [CrossRef]

8. Dowling, B.A., Dart, A.J., Hodgson, D.R., and Smith, R.K. 2000. Superficial digital flexor tendonitis in the horse. *Equine Vet. J.* **32**: 369–378. [Medline] [CrossRef]

9. Ely, E.R., Avella, C.S., Price, J.S., Smith, R.K., Wood, J.L., and Verheyen, K.L. 2009. Descriptive epidemiology of fracture, tendon and suspensory ligament injuries in National Hunt racehorses in training. *Equine Vet. J.* **41**: 372–378. [Medline] [CrossRef]

10. Farris, D.J., Buckeridge, E., Trewartha, G., and McGuigan, M.P. 2012. The effects of orthotic heel lifts on Achilles tendon force and strain during running. *J. Appl. Biomech.* **28**: 511–519. [Medline]

11. Jansen, M.O., van Buiten, A., van den Bogert, A.J., and Schamhardt, H.C. 1993. Strain of the musculus interosseus medius and its rami extensorii in the horse, deduced from in vivo kinematics. *Acta. Anat. (Basel)* **147**: 118–124. [Medline] [CrossRef]

12. Jansen, M.O., van den Bogert, A.J., Riemersma, D.J., and Schamhardt, H.C. 1993. In vivo tendon forces in the forelimb of ponies at the walk, validated by ground reaction force measurements. *Acta. Anat. (Basel)* **146**: 162–167. [Medline] [CrossRef]

13. Kasashima, Y., Takahashi, T., Smith, R.K.W., Goodship, A.E., Kuwano, A., Ueno, T., and Hirano, S. 2004. Prevalence of superficial digital flexor tendonitis and suspensory desmitis in Japanese Thoroughbred flat racehorses in 1999. *Equine Vet. J.* **36**: 346–350. [Medline] [CrossRef]

14. Lam, K.H., Parkin, T.D., Riggs, C.M., and Morgan, K.L. 2007. Descriptive analysis of retirement of Thoroughbred racehorses due to tendon injuries at the Hong Kong Jockey Club (1992–2004). *Equine Vet. J.* **39**: 143–148. [Medline] [CrossRef]

15. Lawson, S.E., Chateau, H., Pourcelot, P., Denoix, J.M., and Crevier-Denoix, N. 2007. Effect of toe and heel elevation on calculated tendon strains in the horse and the influence of the proximal interphalangeal joint. *J. Anat.* **210**: 583–591. [Medline] [CrossRef]

16. Lephart, S.A. 1984. Measuring the inertial properties of cadaver segments. *J. Biomech.* **17**: 537–543. [Medline] [CrossRef]

17. Lochner, F.K., Milne, D.W., Mills, E.J., and Groom, J.J. 1980. In vivo and in vitro measurement of tendon strain in the horse. *Am. J. Vet. Res.* **41**: 1929–1937. [Medline]

18. Meershoek, L.S., and Lanovaz, J.L. 2001. Sensitivity analysis and application to trotting of a noninvasive method to calculate flexor tendon forces in the equine forelimb. *Am. J. Vet. Res.* **62**: 1594–1598. [Medline] [CrossRef]

19. Meershoek, L.S., Lanovaz, J.L., Schamhardt, H.C., and Clayton, H.M. 2002. Calculated forelimb flexor tendon forces in horses with experimentally induced superficial digital flexor tendinitis and the effects of application of heel wedges. *Am. J. Vet. Res.* **63**: 432–437. [Medline] [CrossRef]

20. Meershoek, L.S., Schamhardt, H.C., Roepstorff, L., and Johnston, C. 2001. Forelimb tendon loading during jump landings and the influence of fence height. *Equine Vet. J. Suppl.* **33**: 6–10. [Medline] [CrossRef]

21. Meershoek, L.S., and Van den Bogert, A.J. 2000. Mechanical analysis of locomotion. pp. 305–326. *In*: Equine Locomotion. (Back, W., and Clayton, H. eds.). W.B. Saunders, London.

22. Meershoek, L.S., van den Bogert, A.J., and Schamhardt, H.C. 2001. Model formulation and determination of in vitro parameters of a noninvasive method to calculate flexor tendon forces in the equine forelimb. *Am. J. Vet. Res.* **62**: 1585–1593. [Medline] [CrossRef]

23. Platt, D., Wilson, A.M., Timbs, A., Wright, I.M., and Goodship, A.E. 1994. Novel force transducer for the measurement of tendon force in vivo. *J. Biomech.* **27**: 1489–1493. [Medline] [CrossRef]

24. Pourcelot, P., Defontaine, M., Ravary, B., Lemâtre, M., and Crevier-Denoix, N. 2005. A non-invasive method of tendon force measurement. *J. Biomech.* **38**: 2124–2129. [Medline] [CrossRef]

25. Riemersa, D.J., and Schamhardt, H.C. 1982. The cryo-jaw, a clamp designed for in vitro rheology studies of horse digital flexor tendons. *J. Biomech.* **15**: 619–620. [Medline] [CrossRef]

26. Riemersma, D.J., van den Bogert, A.J., Jansen, M.O., and Schamhardt, H.C. 1996. Influence of shoeing on ground reaction forces and tendon strains in the forelimbs of ponies. *Equine Vet. J.* **28**: 126–132. [Medline] [CrossRef]

27. Stephens, P.R., Nunamaker, D.M., and Butterweck, D.M. 1989. Application of a Hall-effect transducer for measurement of tendon strains in horses. *Am. J. Vet. Res.* **50**: 1089–1095. [Medline]

28. Takahashi, T., Kai, M., Hada, T., Eto, D., Muka, K., and

Ishida, N. 2002. Biomechanical implications of uphill training on the aetiology of tendinitis. *Equine Vet. J. Suppl.* **34**: 353–358. [Medline] [CrossRef]

29. Takahashi, T., Kasashima, Y., Eto, D., Mukai, K., and Hiraga, A. 2006. Effect of uphill exercise on equine superficial digital flexor tendon forces at trot and canter. *Equine Vet. J. Suppl.* **36**: 435–439. [Medline] [CrossRef]

30. Takahashi, T., Yoshihara, E., Mukai, K., Ohmura, H., and Hiraga, A. 2010. Use of an implantable transducer to measure force in the superficial digital flexor tendon in horses at walk, trot and canter on a treadmill. *Equine Vet. J. Suppl.* **42**: 496–501. [Medline] [CrossRef]

31. Thorpe, C.T., Clegg, P.D., and Birch, H.L. 2010. A review of tendon injury: why is the equine superficial digital flexor tendon most at risk? *Equine Vet. J.* **42**: 174–180. [Medline]

[CrossRef]

32. Williams, R.B., Harkins, L.S., Hammond, C.J., and Wood, J.L. 2001. Racehorse injuries, clinical problems and fatalities recorded on British racecourses from flat racing and National Hunt racing during 1996, 1997 and 1998. *Equine Vet. J.* **33**: 478–486. [Medline] [CrossRef]

33. Woo, S.L., Peterson, R.H., Ohland, K.J., Sites, T.J., and Danto, M.I. 1990. The effects of strain rate on the properties of the medial collateral ligament in skeletally immature and mature rabbits: a biomechanical and histological study. *J. Orthop. Res.* **8**: 712–721. [Medline] [CrossRef]

34. Yamamoto, N., and Hayashi, K. 1998. Mechanical properties of rabbit patellar tendon at high strain rate. *Biomed. Mater. Eng.* **8**: 83–90. [Medline]